2

Focused Ion Beam Lithography

Heinz D. Wanzenboeck and Simon Waid
Vienna University of Technology – Institute for Solid State Electronics
Austria

1. Introduction

Optical lithography is the unrivalled mainstream patterning method that allows for cost-efficient, high-volume fabrication of micro- and nanoelectronic devices. Current optical photolithography allows for structures with a reproducible resolution below 32 nm. Nevertheless, alternative lithography methods coexist and excel in all cases where the requirement for a photomask is a disadvantage. Especially for low-volume fabrication of microdevices, the need for a photomask is inefficient and restricts a fast structuring, such as required for prototype device development and for the modification and repair of devices. The necessity of high-resolution masks with a price well above €10k is too cost intensive for the fabrication of single test devices. For this reason 'direct-write' approaches have emerged that are popular for several niche applications, such as mask repair and chip repair. Optical direct-write lithography and electron beam lithography are among the most prominent techniques of direct-write lithography. Less known, but highly versatile and powerful, is the ion beam lithography (IBL) method.

Optical direct-write lithography uses laser beam writers with a programmable spatial light modulator (SLM). With 500 mm^2/minute write speed and advanced 3D lithography capabilities, optical direct-write lithography is also suitable for commercial microchip fabrication. However, with a resolution of 0.6-µm minimum feature size of the photoresist pattern, optical direct-write lithography cannot be considered a nanopatterning method.

Electron beam lithography uses a focused electron beam to expose an electron beam resist. Gaussian beam tools operate with electron beams with a diameter below 1 nm so that true nanofabrication of structures is feasible. A resolution of 10 nm minimum feature size of the e-beam resist pattern has been successfully demonstrated with this method. However, special resists are required for e-beam lithography, that are compatible with the high energy of forward scattered, back-scattered and secondary electrons. A common resist for sub-50nm resolution is polymethylmetacrylate (PMMA) requiring an exposure dose above 0.2 $\mu C/\mu m^2$. For highest resolution (below 20 nm) inorganic resists such as hydrogen silsesquioxane (HSQ) or aluminium fluoride (AlF3) are used, which unfortunately require a high electron exposure dose. Hence, high-resolution electron beam lithography (EBL) is linked to long exposure times which, in combination with a single scanning beam, results in slow processing times. Therefore, this high-resolution method is only used for writing photomasks for optical projection lithography and for a limited number of high-end applications. A resolution to this dilemma may be the use of multi-beam electron tools, as are currently under development. Also electron projection lithography has been under

development but currently all development programmes for a commercial tool have been discontinued.
FIB lithography is similar to EBL, but provides more capabilities. Not only can FIB lithography (i) create a pattern in a resist layer just like EBL, but it is also capable of (ii) locally milling away atoms by physical sputtering with sub-10nm resolution (subtractive lithography), (iii) locally depositing material with sub-10nm resolution (additive lithography), (iv) local ion implantation for fabrication of an etching mask for subsequent pattern transfer and (v) direct material modification by ion-induced mixing.
The ion direct-write lithography combines the high resolution of electron beam lithography with the higher writing speed of optical laser writers. With so-called liquid metal ion sources focusing of the ion beam to a diameter down to 5 nm is feasible. Due to the higher mass of the ions the higher energy of the ion beam allows a faster exposure of resists and thus a higher processing speed. Currently, new ion sources have been developed and also ion projection systems and multi-beam systems are on the verge of commercial introduction, so that this "exotic" technique deserves more consideration for future nanofabrication.
FIB lithography is superior to EBL, as with focused ion beam (FIB) proximity, effects are negligible as no electron backscattering occurs. As a consequence, a higher resolution can be obtained with FIB as the pixel size is roughly equal to the beam spot size and no exposure occurs between pixels, hence allowing a short dwell time on each pixel. With the shorter ion range, weaker forward scattering and smaller lateral diffusion of secondary electrons, FIB lithography reaches a higher resolution than EBL with the same beam spot size. Overall, the higher resist sensitivity to ions increases the throughput in contrast to EBL.
A speciality of ion beam direct-write lithography is the possibility for resistless structuring. The application of a resist layer is not possible on non-planar samples, such as prestructured wafer surfaces or three-dimensional samples. If a resist layer can be applied, small structures are typically only feasible with ultrathin resist layers with a homogeneous thickness below 100 nm. The ion beam can also be used for direct-write implantation of direct-write milling of patterns in order to fabricate structures. The implantation of ions originating from the ion source itself can be used to fabricate locally doped hardmask layers that can be used for pattern generation in a subsequent selective etching process. This approach will be described in detail in section 4.3. The straightforward approach for pattern generation is the direct-write milling with a focused ion beam. The kinetic energy of accelerated ions may be used for physical sputtering of the substrate. With a focused Ga^+ ion beam of less than 5 nm diameter, structures with 30 nm features have been realized. This processing alternative will be described in detail in section 4.1. A sub-version of direct-write milling with an ion beam is the gas-assisted etching and the beam-induced deposition. The physical milling by the ion beam is complemented by a chemical reaction locally triggered by the energy of the ion beam. With gas-assisted etching, an etch gas is added that can react with the substrate to form a volatile etch product. With beam induced deposition a precursor gas is added that locally decomposes on those substrate areas scanned by the ion beam. From this ion beam-induced deposition, a solid material structure is formed. This is an 'additive' direct-write lithography technique.

2. Ion-solid interaction

The fundamental process of resist-based IBL is the ion-induced change of the resist. Typically, ion beam resists are used as negative resists experiencing a decrease of solubility

of the ion exposed area due to ion-triggered reactions. Also with ion beam-induced etching and ion beam-induced deposition, a chemical reaction of surface species is the underlying mechanism of this structuring approach. For this reason, the ion-solid reaction shall be taken into closer examination.

Ion interaction with solid can be separated in elastic and inelastic collisions and in electronic interactions. Ion-atom as well as ion-electron collisions are typically treated as binary collisions. For the treatment of ion-atom collisions, a lower energy limit of 10 to 30 eV has to be considered. At lower energies, many body interactions are also a relevant mechanism, which is up to now widely neglected in literature due to its complexity (Eckstein, 1991).

Elastic collisions between ions and atoms of the substrate (or resist) are responsible for (i) beam broadening by scattering, (ii) amorphization of the target substrate, (iii) ion implantation into the target substrate, and (iv) sample physical sputtering. Both forward scattering and backward scattering lead to a broadening of the ion beam propagating in matter. As a practical consequence, this reduces the resolution when exposing a resist layer. Ions impinging into the substrate lead to the secondary effects of atomic mixing, which results in amorphization of crystalline samples, in the intermixing of resist and substrate at the interface and also implantation of the primary ions (often as an element) into the substrate. With photoresist, this may also lead to problems with later removal, as ion-implanted resists display a higher etch resistivity in plasma ashers. In the special case of sputtering, the substrate material is removed as a consequence of elastic collisions. The incident ions transfer their momentum to the target atoms within a collision cascade region. Atoms from the substrate surface may be ejected as a sputtered particle if it receives a kinetic energy that is sufficient to overcome the surface binding energy (SBE) of the target material. This effect is used for direct-write structuring by milling without any resist.

The ion beam may also be used to initiate chemical reactions. For this process, energy has to be converted from kinetic energy into other types of energy, such as bond dissociation energy. Such inelastic collisions involve an energy transfer either to electrons of the substrate (‘electronic stopping’) or an energy transfer to other nuclei or atoms of the substrate.

About two thirds of the dissipated energy is transformed into kinetic energy of so-called δ-electrons. Heavy ions dissipate their energy along their trajectories ionizing target atoms and producing free electrons. Around the ion's trajectory, secondary and tertiary ionization processes occur. Inelastic processes may lead to ionization of atoms involving also secondary electron emission. The secondary electrons are also subscribed a significant role in bond breaking mechanisms as a consequence of ion irradiation. Secondary electrons have energy between 1 and 50 eV corresponding to the energy range required to break molecular bonds (sigma and pi bonds). Other inelastic processes involve loss of kinetic energy by emission of photons including emission of x-rays, of Bremsstrahlung, or of Čerenkov radiation. Finally, heating, luminescence, shock wave or phonon excitation are other energy-loss mechanisms affecting not a single atom but rather an entire volume of the irradiated substrate.

Chemical reactions of the resist layer or of the substrate are induced by effects of inelastic collision of the primary ions. For chemical reactions of the resist layer, primarily the secondary electron-induced bond dissociation or the radical production is considered as a relevant mechanism. The low-energy secondary electrons (generated by ion-matter interaction) can expose a resist layer for lithography analogous to the secondary electron induced reactions used in EBL. Hence, electron beam resists can also be used as FIB lithography resists.

FIB lithography has the advantage of (i) a higher resolution due to the absence of proximity effects and (ii) a higher resist sensitivity. As no electron backscattering exists, the pixel size with FIB lithography is equal to the ion beam spot size and thus can be much higher than with EBL. As a primary ion can release up to 200 secondary electrons (Dietz & Sheffield, 1975), while a primary electron can release less than 2 secondary electrons (Hoyle, 1994) the exposure speed with ion lithography can be up to a factor of 100. On the other hand, FIB lithography resists suffer from a restricted exposure depth in the resist and from contamination of the resist by source ions. To circumvent larger structures resulting from the restricted exposure depth, a thin resist layer can be used, but this makes subsequent etching processes or lift-off processes more difficult. The contamination of the resist is especially problematic, if organic resists are removed by plasma ashing and the inorganic contaminations remain on the surface.

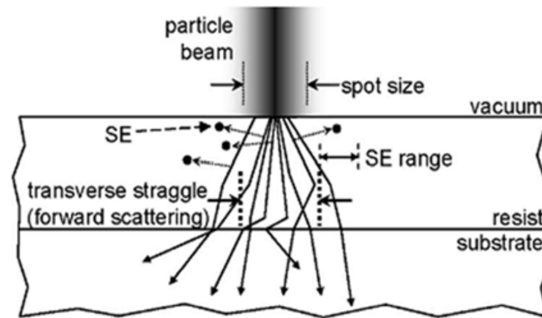

Fig. 1. Factors limiting resolution of IBL. A focused ion beam irradiates a resist layer on a substrate. The three factors limiting resolution are (i) spot size of the beam (ii) ion scattering and (iii) secondary electron emission.
Reprinted with permission from Winston D. et al., 2009. Scanning-helium-ion-beam lithography with hydrogen silsesquioxane resist. JVST B 27(6), 2702. Copyright 2009, American Vacuum Society.

Ion beam lithography has repeatedly been successfully used for exposing resist layers.
Structural modification of the resist, including chain scission, cross-linking, double-bond formation, molecular emission, changes in molecular weight distribution, and so forth are due to ion irradiation of polymers (Calcagno et al., 1992). The degradation of PMMA by proton beam irradiations for resist applications has been analyzed by Choi et al. (Choi et al., 1988). Even though the energies of the radiation sources varied considerably (up to 900 keV for H3+), they observed a 1-to-1 correspondence of loss of ester groups and generation of double bonds in the polymer chains for all radiation types.
Horiuchi et al. (Horiuchi et al., 1988) have achieved 200 nm line width in PMMA using a He+ ion beam. Using a Ga+ beam Kubena et al. (Kubena et al., 1989) could even demonstrate sub-20 nm line width in PMMA. The higher energy transmission by the ions allows for faster exposure of resists by ion beams so that also resists requiring prohibitively high electron doses with EBL can be used in IBL. Therefore, inorganic high-resolution resists such as hydrogen sesquioxane (HSQ) and aluminium fluoride can also be used. Hydrogen silsesquioxane (HSQ) is a negative-tone resist that cross-links via Si–H bond scission (Namatsu et al., 1998). The energy of a Si–H bond is roughly 3 eV and can be broken by secondary electron energy. Van Kan et al. (van Kan et al., 2006) have successfully demonstrated 22 nm line width in HSQ using a 2 MeV H_2^+ beam.

3. Ion beam equipment

For structuring with an ion beam, two complementary approaches have to be distinguished. The equipment setup differs among those approaches described in Table 1. Yet, the experimental setup always includes an ion source and an ion optical system consisting of electrostatic lenses and electrostatic deflectors. For ion optics, only ions of a specific mass and of a specific energy can be used for the focusing optics. From the use of ions for structuring 'resist-based' and 'resistless' methods can be distinguished.

Beam type	Scanning beam	Broad, collimar beam
Method	'direct-write technique'	'projection technique'
Mask	maskless (structure by pattern generator)	aperture mask

Table 1. Structuring approaches using an ion beam

3.1 Ion sources

The core component of an ion beam system is the ion source. Development of ion sources initially was motivated by mass spectrometry and ion implantation for semiconductor manufacturing. Only with the emerging resolution limits of optical lithography particle beam methods became interesting for nanostructuring. For using a focused beam, a point source is required, while broad beams can also use ion sources emitting ions over a larger area. Four basic ion source types are described below:

1. **Electron bombardment ion sources.** An electron beam is directed onto a gas. Under electron bombardment, the gas molecules in the irradiated volume become ionized. Hence, the ions are not emitted by a localized source. The resulting ion current is rather small but typically has a small ion energy spread. Due to the low currents these sources are not used for ion lithography but find their application in mass spectrometry (Dworetsky et al., 1968). This source has been used successfully to produce low-energy beams of noble gas ions, such as He+ and Ar+, without measurable contamination, as well as for H_2+ and N_2+.
2. **Gas discharge ion source.** The ions are created by plasma or by electric discharge. Typically ions are generated by capacitively coupled plasma, inductively coupled plasma or by microwave-induced plasma. An alternative are glow discharge of a gas at low pressure or spark ionization of a solid sample. As ions from gas discharge are emitted over a larger gas volume, they are not point-sources and are therefore not suitable for focused beams. However, gas discharge ion sources produce a high ion current and are therefore interesting sources for ion lithography based on the projection method. These sources are also widely used in high-energy accelerators and ion implanters for semiconductor manufacture. A widely used type is the duoplasmatron. First, gas, such as argon, is introduced into a vacuum chamber where it is charged and ionized through interactions with the free electrons from the cathode. The ionized gas and the electrons form a plasma. By acceleration through two highly charged grids, ions are accelerated and form a broad ion beam.
3. **Field ionization source.** These sources operate by desorption of ions from a sharp tip in a strong electric field. Typically, gas molecules are adsorbed on the surface of a sharp needle tip and are directly ionized in the high electrical field prevailing at the tip apex.

Due to the point-like emission of ions from a single spot, the focusing to a beam with an ultra-small diameter is feasible. The adsorbtion of gas on the tip may be enhanced by cryostatic cooling of the tip. The focused ion beam may be used for a field ion microscope and typically non-reactive ions, such as noble gas, ions are used.

4. **Liquid metal ion source (LMIS).** The LMIS operates by desorbtion of metal ions from liquid metal under a strong electrical field. Typically a thin needle or a capillary is wetted by a thin film of liquid source metal, which has been heated to the liquid state. Typically, gallium (m.p. 29,8°C) or indium (m.p. 156,6°C) or Be-Si-Au alloys ($Au_{70}Si_{15}Be_{15}$) are employed. A Taylor cone is formed under the application of a strong electric field. The force acting onto the needle due to the electric filed shapes the cone's tip to get sharper, until ions are produced by field evaporation. For emission of ions, a threshold extractor voltage (for Ga 2kV) is required. For an alloy source, an energy separator is needed to filter out one ion species. Liquid metal ion sources are particularly used in focused ion beam microscopes. The emission angle is around 30°. The angle distribution of emission current is rather uniform. Energy spread of emitted ions can be large (>15V) resulting in a large chromatic aberration.

Depending on whether a resist layer is used or resistless structuring is performed, patterning with an ion beam opens up different structuring capabilities, as shown in Table 2.

	Single focused beam	**Broad beam**
	Scanning beam ➔ maskless	Projection ➔ requires mask
Resist	Direct-write exposure of resist	Projection exposure
Resistless	Direct-write Milling or Direct-write Deposition or Direct-write Etching	Projection milling

Table 2. Resist-based and resistless patterning approaches with an ion beam

Depending on the selected source type focused beam systems and broad beam systems also have to be distinguished as depicted in Table 3.

		Focused beam	**Broad beam**
		High resolution	Low resolution
Single beam	Sequential writing → slow	Ga LMIS He-LIS	Plasma source
Multi-beam	Parallel writing → fast	Plasma source with aperture plate and projection optics	-

Table 3. System configurations with ion beam tools

3.2 Ga ion microscopes

Focused ion beam tools using a liquid metal ion source for Ga ions are currently the state of the art, because this ion beam can be made very small and therefore resembles a perfect tool for nanofabrication. The Ga ion beam can be focused below 5nm diameter, as the ion source is almost an ideal point source. The original W wire is not sharp and may have a tip radius of more than 1 µm. The sharp tip is formed by the liquid metal induced by the electric field.

This Taylor cone of liquid metal results in a very high electric field at the cone apex, which is required for field emission of the ions.

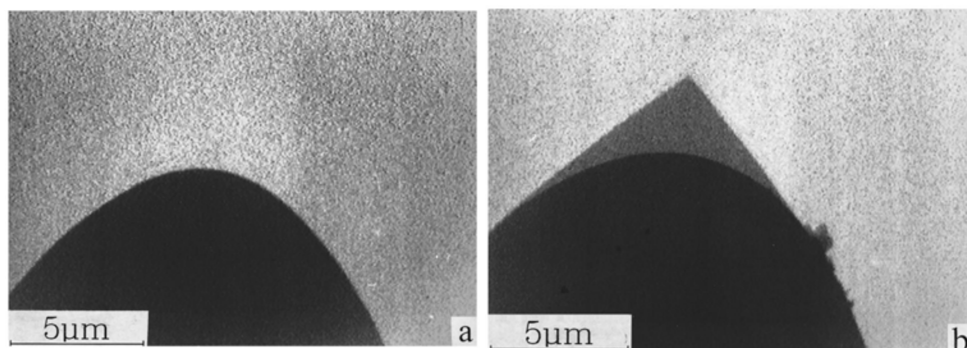

Fig. 2. Shape of the emitter tip coated with a liquid AuGe alloy (a) without Taylor cone; (b) with Taylor cone.
Reprinted with permission from Driesel W., Dietzsch C. & Muhle R., 1969. In situ observation of the tip shape of AuGe liquid alloy ion sources using a high volt transmission electron microscope. JVST B 14(5), 3367. Copyright 1969, American Vacuum Society..

The ion beam is used for imaging (Orloff et al., 1996), local implantation (Schmidt et al., 1997), physical milling (Giannuzzi & Stevie, 1999), gas-assisted etching (Utke et al., 2008), localized deposition (Matsui et al., 2000) and for exposure of resist layers (J. Melngailis, 1993) (Lee & Chung, 1998) as extensively described in literature (Tseng, 2005); (Giannuzzi & Stevie, 1999) (Jeon et al., 2010) (Tseng, 2004) and is therefore not further discussed here in detail.

3.3 He ion microscope

'Heavy' ions, such as Ga+, may displace and scatter atoms in the substrate so much that device performance suffers. The He ion beam offers a new alternative. Helium ions are more massive than electrons by over three orders of magnitude and thus diffract less around apertures. Thus, smaller apertures are possible in a helium ion column than in an electron column, and this enables a smaller spot size. The specified spot size for a Zeiss Orion Plus helium ion microscope is 0.75 nm at an accelerating voltage of 30 kV. The first commercial helium ion microscope was introduced in 2006 (B. W. Ward et al., 2006) and by now has reached a maturity so that edge resolutions of <0.35 nm have become routinely possible.
As ion source a cryogenically cooled metal needle with a tip in the shape of a three-sided pyramid is used. The He+ source can be cooled to around 80 K, which resembles a point source that can be focused. When gun temperature exceeds 95 K, this structure is unstable, meaning source size and thus brightness may become compromised at higher temperatures A small quantity of helium is admitted in the vicinity of the sharp tip in the shape of a three-sided pyramid. The apex of the pyramid consists of a set of three atoms, the trimer. The injected helium is then polarized by the large electric field and He atoms accelerate towards ionization area near the three topmost atoms. Only in this restricted area at the pyramidal tip does ionization take place. The charged He ions from one emitter atom are selected and are accelerated into the ion column to produce the focused electron beam. The ion optics should theoretically operate around unity magnification.

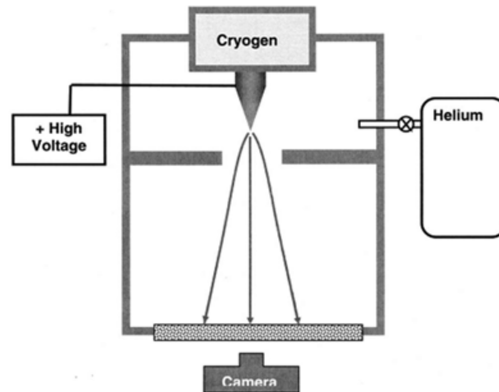

Fig. 3. Field ion microscope in its simplest form consists of a cryogenically cooled tip, biased to a high voltage. When the imaging gas is admitted, a pattern is visible on the scintillator. Reprinted with permission from Ward B.W., Notte J.A. & Economou N.P., 2006. Helium ion microscope: A new tool for nanoscale microscopy and metrology. JVST B 24(6), 2871. Copyright 2006, American Vacuum Society.

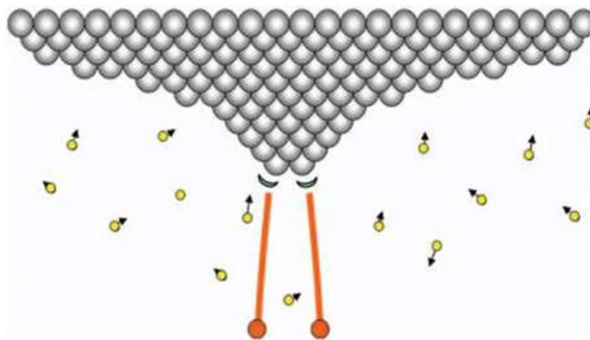

Fig. 4. Spherical tip after the atoms have been rearranged to form a three-sided pyramid. Now the ionization disks exist only over the topmost three atoms.
Reprinted with permission from Ward B.W., Notte J.A. & Economou N.P., 2006. Helium ion microscope: A new tool for nanoscale microscopy and metrology. JVST B 24(6), 2871. Copyright 2006, American Vacuum Society.

The depth of field with a He ion microscope is correspondingly five times larger as the convergence angle is typically five times smaller than an SEM. Also the diffraction curve is over two orders of magnitude smaller compared to the SEM. Consequently, an ideally focused spot may have a spot size down to 0.25 nm.
With current systems, the virtual source size is smaller than 0.25 nm while providing a brightness of approximately 10^9 Acm^{-2}. Measurements have shown an angular beam intensity of 0.5–1 μAsr^{-1} and an energy spread of 1 eV. (R. Hill & Faridur Rahman, 2010).
The interaction of the He ion beam with the sample is significantly different than with either an electron beam or a Ga+ ion beam. Versus using electrons, He ions are advantageous by the strongly reduced diffraction effect which enables a tremendously increased resolution of

smaller structures. He ion microscopy is highly suitable for imaging of insulating samples and biological samples. The scanning helium ion microscope can also be used for diffraction imaging in transmission mode (J. Notte 4th et al., 2010). This way, crystallographic information can be provided in the form of thickness fringes and dislocation images. This mode allows the recording of high-contrast images of crystalline materials and crystal defects even at modest beam energies.

Helium ion microscopy has already been successfully used for resist-based structuring and the feasibility of 6nm features has been demonstrated (Sidorkin et al. 2009). Ion beams may also be used for sample sputtering, but the light He ions have a very low yield. Yet, successful milling of graphene structures by He ion microscopes has been shown by R. Hill & Faridur Rahman (2010) and Bell et al. (2009). As with Ga ion microscopy the ion beam may also be used for gas-assisted deposition or etching. The fabrication of a W pillar with an average diameter of 50 nm grown by deposition in the He ion microscope has been demonstrated. This deposited pillar was 6.5 µm high and had a height to width aspect ratio of 130:1 (R. Hill & Faridur Rahman 2010). Also 10 nm wide nanowires have been deposited and sub-10 nm cuts in Au have been performed with a focused helium ion beam (Livengood et al. 2011)

3.4 Ne ion microscope

The development of ion microscopes with heavier noble gas ions is currently underway (Livengood et al., 2011). Utilizing neon ions extends the capabilities of high-source brightness technology. The neon ion source will also use the trimer-gas-field ion source used in the He ion microscope.

For a stable GFIS source it is necessary that other gas contaminants have lower ionization energy than the noble gas ions, otherwise ionization of contaminants might also occur. The resulting contamination of the source region would contaminate the trimer trip region. Besides helium (24.5 eV), neon (21.6 eV) is the only noble gas with an ionization energy significantly higher than that of contaminants such as O, (13.7 eV), N (14.5 eV) and CO_2 (13.8 eV). Therefore, Ar (15.8 eV) Kr and Xe (11.1 eV) are less suitable ions for this process.

With a test system the beam diameter was determined to be 1.5 nm at 28 kV, with a sputter yield around 1 atom per incident ion for Si and 4 atoms per incident ion for Cu. In comparison to a gallium FIB this is by a factor of 2x lower. In comparison to the light helium ions this is by a factor of 100x higher.

Nanomachining tests performed in a 600 nm SiO2-CDO dielectric stack and in 30 nm Cr–SiO_2 using 24 kV beam energies (1 pA beam current) have achieved smallest via a 40 nm at the mid-point and 30 nm at the base, with a depth of 240 nm (6:1 aspect ratio via). These first results indicate structure widths larger than expected and side wall profiles poorer than expected, so that further improvements have to be implemented. The benefit of a Ne ion beam will be in the field of milling, as the heavier ion species is more suitable for material modification such as ion milling or beam-induced deposition or etching.

3.5 Ion projection systems

From an industrial viewpoint, a major deficit of focused ion beam systems is the sequential scanning with a single beam resulting in a very low sample throughput. For this reason projection systems have been developed using a stencil mask (Hirscher et al., 2002). A broad helium beam is extracted from a plasma source. An ExB mass filter selects only the desired He ion species. The ion projection lithography (IPL) system uses electrostatic ion optics for

reduction printing of stencil mask patterns to a magnification factor of 4. Monitoring the position of the ion beam for correction of the projected image was achieved with a pattern lock system which consists of (i) detectors measuring the position of beamlets, (ii) transputer-based controllers and (iii) beam control elements.

An ion projection lithography system for exposure of the Shipley XP9946 resist family allowing for very high resolution of 50 nm was developed. A high pattern collapse probability was experienced at high aspect ratios. Required ion doses varied with the composition of the resist and were in the range of 1.4 down to 0.12 $\mu C/cm^2$. Alternatively sensitivity adjustment by a variation of the photo acid generator (PAG) was achieved.

3.6 Multi-beam systems

Based on an ion projection concept using a stencil mask, further development efforts of IMS Nano have brought forward an ion multi-beam system. This multi-beam system features a programmable aperture plate with integrated CMOS electronics (Hans Loeschner et al., 2010). This aperture plate is equipped with deflection electrodes and a blanking plate. A beam deflection of 300 mrad from the axis is sufficient to filter out a beamlet. By blanking through one aperture a single beam can be individually switched on and off. The produced pattern of individually switched ion beams can be demagnified leading to a 200x pattern reduction.

As ion source a broad beam generated from plasma was used. The gases ionized ranged from hydrogen H_3^+ to Argon (Koeck et al., 2010).

Using 10 keV H^+ ions, a 20 nm thick layer of the inorganic photoresist hydrogen silsesquioxane (HSQ) was exposed. For this purpose the sample was irradiated by 43.000 beams with exposure dose of 12 mC/cm2. Tetramethylammonium hydroxide (TMAH) was used for resist development. After development, an effective 15 nm half-pitch (hp) resolution in 50 nm HSQ resist could be confirmed (Hans Loeschner et al., 2010). Development in NaOH/NaCl required a 3.3x higher exposure dose but longer exposure led to reduced shot noise influence on line edge roughness (LER).

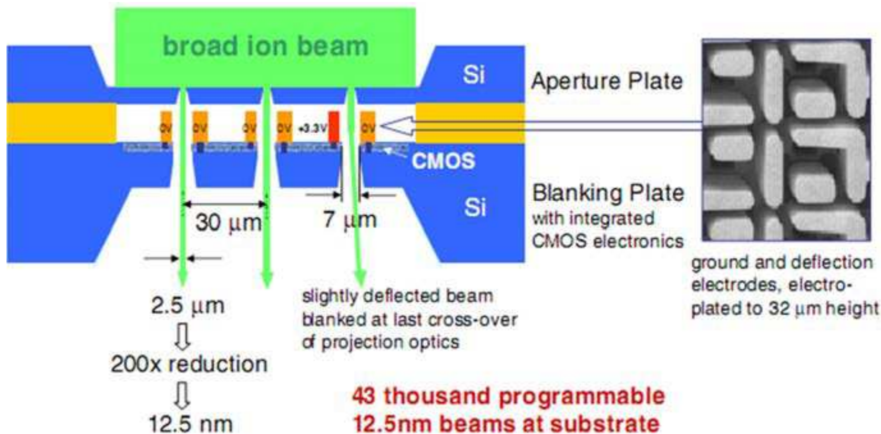

Fig. 5. Schematics of a 43k-APS unit of the IMS system providing 43 thousand programmable beams.

Reprinted with permission from Loeschner Hans, Klein C. & Platzgummer Elmar, 2010. Projection Charged Particle Nanolithography and Nanopatterning. JJAP, 49(6), 06GE01..

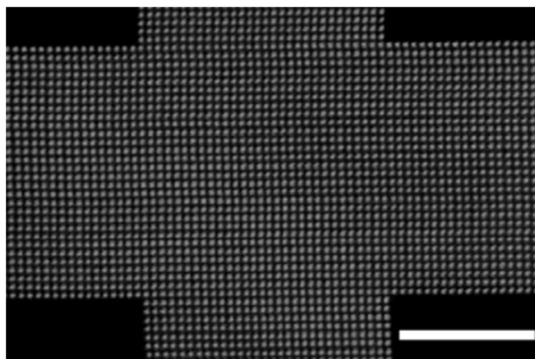

Fig. 6. SEM views of a dot array with 12.5 nm half-pitch features. HSQ was developed in NaOH/NaCl. The scale bar is 400 nm.
Reprinted from Publication Muehlberger M. et al, Nanoimprint lithography from CHARPAN Tool exposed master stamps with 12.5 nm hp, Microel. Eng. 88/8 2070, Copyright 2010, with permission from Elsevier.

This approach has been successfully used to pattern high-resolution patterns with 12.5 nm half-pitch in inorganic HSQ resist and to replicate this pattern by nanoimprint lithography (Muehlberger et al., 2011)

4. Lithography

Lithography is employed to define patterns inside a target material. Using an FIB, a multitude of processing techniques exists to achieve this goal. Similar to photolithography it can be achieved by exposing a resist material using the ion beam. However, with ions, patterns can also be defined by physically sputtering the target atoms (FIB milling), by triggering chemical reactions inside an adsorbed layer of a precursor gas (gas-assisted processing) and by ion implantation.
Among these techniques the most prominent are FIB milling and gas-assisted processing. They are employed for optical mask repair (Yasaka et al., 2008), circuit editing (CE) (Boit et al., 2008), transmission electron microscope (TEM) sample preparation and rapid prototyping (Persson et al., 2010). We will discuss these techniques only briefly since they are already well described and reviewed elsewhere (Reyntjens & Puers, 2001) (Utke et al., 2008). Instead we will focus on the less prominent FIB patterning techniques.
In the following sections we will review the work carried out on resist-based IBL and discuss the reasons for its failure as well as its chance of resurrection. Further we will present our findings on patterning using ion implantation with a focus on 3D nano patterning. Finally, we will introduce a new technique, called direct hard mask patterning (DHP) which combine the advantages of FIB milling with the speed of resist-based lithography.

4.1 FIB milling and gas-assisted processing

When an ion hits the target, surface elastic and inelastic scattering processes will take place. While inelastic processes are responsible for the generation of photons and secondary electrons, elastic scattering will transfer kinetic energy from the ion to the target atoms (Orloff et al., 2002). This kinetic energy transfer will cause the displacement of the target

atoms and trigger a recoil cascade whereby kinetic energy is transferred from one atom to another by elastic scattering processes.
When the recoil cascade induced by the incident ion reaches the surface the target atoms at the surface may gather sufficient energy to leave the surface and enter the surrounding vacuum. The atoms are then either re-deposited or removed from the vacuum chamber by the pumping system. This material removal process is called milling.
How many target atoms a single ion is able to remove is largely dependent on the target material, the ions species, its energy and the angle of incidence of the ion beam. E.g. a 30keV Ga ion may eject 2 to 3 Si atoms. A 25keV Ga ion may also eject 23 Au atoms (Utke et al., 2008).
This milling process can be easily applied to almost any material and permits patterning down to the sub-100 nm regime. Due to its large material independence and high achievable resolution this process is commercially employed for transmission electron microscope (TEM) sample preparation. Due its ease of application and versatility, this process is often employed for rapid prototyping in research. Due to the high ion doses required for patterning only small areas can be patterned by FIB milling if processing times ought to remain within reasonable limits.
The energy transfer from the incident ion to the target may also be transferred to molecules adsorbed on the target surface. This may trigger a chemical reaction. Possible chemical reactions include the decomposition of adsorbed molecules and reaction of adsorbed molecules with the target atoms. This FIB-induced reaction process is illustrated in Figure 7. The energy transfer mechanism from the ion to the adsorbed molecule is not yet fully understood. However, it is commonly agreed that it can be mainly attributed to the same recoil cascade which causes milling. Alternative explanations include secondary electron and local heating.
The decomposition products may be solid and thus deposited on the target surface, or volatile and thus be removed by the pumping system. By the choice of appropriate substances one may induce the local deposition of specific materials, e.g., metals may be deposited from appropriate metal organic precursors. This process is called gas-assisted deposition (GAD).
GAD is commercially employed for rewiring of integrated circuits in circuit editing (CE) (Boit et al., 2008), to protect the specimen surface of TEM samples during preparation by FIB milling and to correct void defects on photo masks (Boit et al., 2008).
The energy transferred to the target surface may trigger a reaction of the precursor with the target material. If the reaction product is volatile this will cause local etching of the target. This is mainly achieved by supplying light, reactive species such as halogens or halogen compound onto the surface. This process is called gas-assisted etching (GAE).
The etching efficiency of the GAE process is dependent on the target material. Thus, this can be employed to locally remove one specific material. E.g., the addition of XeF_2 will increase the removal rate of SiO_2 by a factor of nine compared to FIB milling while the removal rate of most metals (e.g., Al) will not be altered. This can be employed to remove a SiO_2 dielectric layer while mostly keeping Al interconnects intact. GAE is employed for selective removal of material in CE and for the selective removal of Cr in photo mask repair (Utke et al., 2008).
The chemical etching will also increase the removal rate compared to milling. This may be employed to increase processing speed and to minimize contamination and amorphization of the target material.

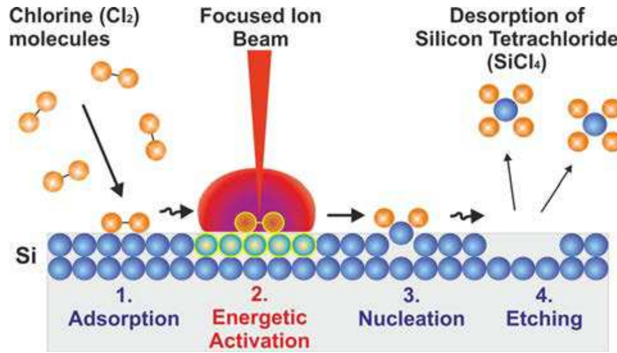

Fig. 7. Schematic illustration of the FIB-induced etching process

4.2 Resist-based lithography

The typical process flow for resist-based IBL is identical to EBL and is illustrated in Figure 8. The pattern definition is performed by the chemical modification of the resist irradiated by ions. The key elements in the process are thus the employed resist and its interaction with the beam employed for exposure.

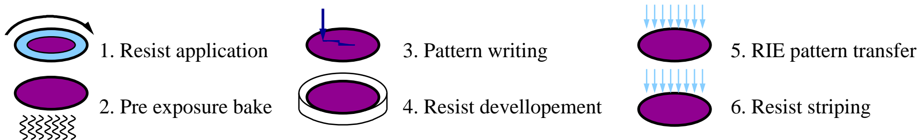

Fig. 8. Typical process flow for resist-based IBL

The resist-based IBL was developed after EBL and thus most resist materials employed in IBL were first employed for EBL and then found suitable for IBL. However, not every material suitable for EBL can be employed for IBL without restriction. Due to the different interaction of ions with resists compared to electrons, the resist properties may change significantly.

How a resist material behaves under ion beam irradiation largely depends on the form of energy deposition. Ions with a low mass to energy ratio deposit their energy mainly by electronic effects. For ions with high mass to energy, the energy deposition is mainly due to nuclear stopping (Gowa et al., 2010).

In the case of electronic energy deposition, resist materials behave similar to what is known from electron beam lithography. The energy dissipated into the resist following exposure leads to chemical damage of the polymer bonds, such as chain scission for positive resist and cross-linking in case of negative resist (Ansari et al., 2004). However, the ion resist interaction is much stronger for ions and will thus result in increased resist sensitivity. E.g., spin on glass (SOG) was found to be 500 times more sensitive to 30keV Ga ions than to electrons (Taniguchi et al., 2006).

Although most resists are more sensitive to ion irradiation than to electron irradiation, this does not imply a higher patterning speed. The practical patterning speed depends on a large number of parameters including source brightness properties of the employed optics and required resolution. Depending on the specifications, either EBL or IBL may be faster. Due

to the availability of higher current densities and the variable shape beam (VSB) writers EBL usually wins this battle.
For low-energy and high-mass ions resist behavior may change severely compared to EBL. It was shown that, for low-energy Ga ions, several positive resists behave as negative resists when irradiated with a high fluency or high flux ion beam (Gowa et al., 2010). This behavior is attributed to cross-linking induced by the radicals liberated by the incident ions (Gowa et al., 2010).
At sufficient ion doses also ion implantation into the resist may be an issue, but can also be employed for patterning. Sufficiently high concentrations of Ga implanted into a resist can protect it from being developed or etched. This fact was employed in combination with a DNQ/Novolak-based resist to permit positive/negative patterning in one exposure step. Weather a feature is exposed positively or negatively is solely dependent on the ion dose (K. Arshak et al., 2004).
During IBL a significant part of the employed ions may be implanted into the substrate. This may be unacceptable in occasions where the substrate is sensitive to defects or doping, e.g., in semiconductor device fabrication. The issue may be circumvented by employing a double-layer resist system, whereby the second layer acts as an ion absorber (Hillmann, 2001).
Beside 2D patterning, resist-based 3D patterning using a FIB was also demonstrated (Hillmann, 2001) (Taniguchi et al., 2006). For this purpose, a positive resist is employed and the depth to which the resist is removed by the developer is dose dependent. Due to the absence of the proximity effect (Hillmann, 2001) this technique permits fast 3D nano patterning with high lateral resolution.
Light ions with large energies may pass thick resist materials with little deviation from their trajectory thus permitting the creation of high aspect ratio features. Due to the large impact of the ion energy and mass, the penetration depth of ions into the resist must always be considered and the resist thickness must be chosen appropriately.
At high resist sensitivities, e.g., when using chemically amplified resists (CARs) resolution and edge roughness may be limited by shot noise (Rau, 1998). Rau found that using a CAR feature printing down to an average of 7 ions was possible, but very unreliable. At an average dose of 28 ions per feature, 98% of all features were printed.
Beside classical organic resists also alternative materials are employed for FIB lithography. The change in the crystalline phase of MoO3 and WO3 (Hashimoto, 1998) was successfully used for patterning. The intermixing of the Ag2Se/GeSe2 bilayer system caused by ion bombardment proved also to be a viable patterning technique (Wagner, 1981). Self-development was shown using two materials, namely AlF3 (Gierak et al., 1997) and nitrocellulose (Harakawa, 1986).
Resist-based focused IBL was studied extensively in the 1980s (Gierak et al., 1997). FIB devices for resist-based FIB lithography were put on the market and the impact of ion irradiation on resist materials was investigated. In the end, IBL could not supersede EBL and the commercialization efforts for these specialized devices were stopped by most companies. The introduction of multi beam and high-resolution FIB systems (Elmar Platzgummer & Hans Loeschner 2009) might now lead to a renascence of resist-based FIB lithography.

4.3 3D patterning by ion implantation

During ion bombardment, ions are implanted into the irradiated substrate. Depending on their mass and energy they will come to a rest in deeper or shallower regions. If the depth in

which the ions come to rest is sufficiently narrow and if a sufficient number of ions are implanted they may form a thin layer of highly doped substrate material and locally change its chemical properties.
For the very common material system gallium on silicon a SRIM (Ziegler, 2004) simulation quickly reveals a projected range of 28 nm at 30keV ion energy. Starting from an ion dose of $2 \cdot 10^{15}$ cm^{-2} (Chekurov et al., 2009), a change in the reactive ion etcher (RIE) etch speed of Si inside doped areas is noticed for fluorine-based plasmas. Only recently it was discovered that by modulating the ion dose, the time the highly doped layer is able to withstand the etching can also be modulated (Henry et al., 2010).
The dependence of the etch depth from the applied Ga dose may be employed as an effective way for 3D patterning. The process flow is illustrated in Figure 9. It consists of two steps: (i) Implantation and (ii) Pattern transfer using RIE. The key parameters for the process are: (i) The implantable Ga quantity in dependence of the scan parameters and (ii) The dependence of the etch depth on the implanted Ga quantity and on the etch parameters. For effective patterning these parameters have to be optimized.

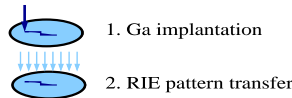

Fig. 9. Process flow

We measured the implantable Ga in dependence of the scan parameters by using EDX. Since EDX can only measure the relative Ga content, a method was needed to calculate the implanted absolute Ga quantity. We found that the dependence of the measured Ga quantity from the applied Ga quantity fitted well to the exponential function in eq. 1. Herby d_m denotes the measured Ga quantity, d_i is the applied Ga quantity and A and B are fit parameters.
Under the assumption that for low ion doses the implanted Ga dose is proportional to the applied Ga dose one can calculate the proportionality factor between measured and applied Ga dose from the fit parameters. The implanted Ga quantity in physical units D_m can thus be calculated using eq. 2.

$$d_m = Be^{Ad_i} \tag{1}$$

$$D_m = \frac{1}{AB} d_i \tag{2}$$

The measured Ga quantity in dependence of the applied Ga quantity for different ion energies is shown in Fig. 12. We find that at low implantation doses, the measured implantation dose is proportional to the applied Ga dose, while at higher implantation doses, the implanted Ga is also removed due to sputtering and the implanted ion dose saturates. The maximum implantable Ga quantity is dependent on the ion energy and becomes higher with increasing energy. The implantation efficiency for 30keV Ga ions is

summarized in Table 4. One will tend to maximise the implantation efficiency and thus choose sufficiently low implantation doses.
Besides the impact of the ion energy, we also measured the influence of scanning speed and ion current on the implanted dose (not shown). At doses below 100pC/µm² and 30keV ion energy we find that the effect of these parameters on the implanted Ga quantity is negligible. In practice, one will necessarily avoid higher implantation doses due to the low implantation efficiency.

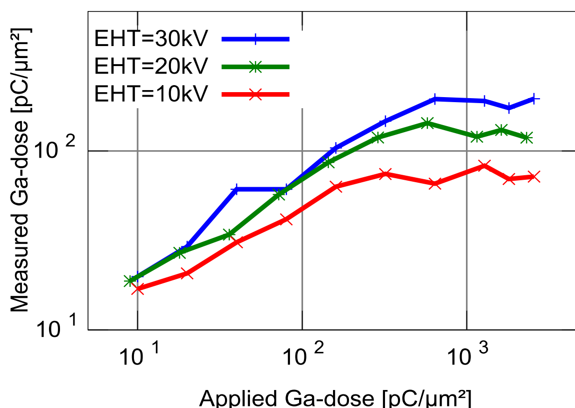

Fig. 10. Impact of the applied Ga dose on the effectively implanted ion dose. The indicated measured ion dose shown was calculated from the measured relative ion dose as described in the text.

Ion dose	**Implantation efficiency**
100pC/µm²	75%
200pC/µm²	60%
300pC/µm²	50%
500pC/µm²	36%

Table 4. Effect of the ion dose on the implantation efficiency at an ion energy of 30keV

For the RIE pattern transfer, the dependence of the etching depth on the applied Ga dose is of importance. We measured the dependence for three gas compositions, namely SF_6 + Ar, SF_6 + O_2 and SF_6 + $SiCl_4$. The first of these gas compositions was found to be the most interesting for 3D patterning. The SF_6 + $SiCl_4$ gas composition was found to be useful to suppress the masking effect of implanted Ga.
The resulting etch depth in dependence on the applied Ga dose for the SF_6+Ar plasma is shown in Fig. 11. We find that depending on the plasma composition the sensitivity of the etch depth on the applied Ga dose may be modulated. To optimize the overall process for speed one will tend to choose a gas composition which minimizes the required implantation dose. However, the process with the highest dose sensitivity will also exhibit the highest sensitivity against dose variations. Thus, in practice, one will have to make a trade-off between patterning speed and precise height control.

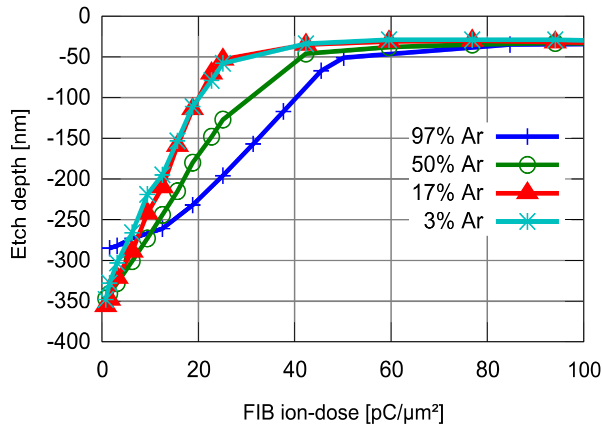

Fig. 11. Impact of the implanted ion dose on the etch depth. The etch gas was composed of Ar and SF_6.

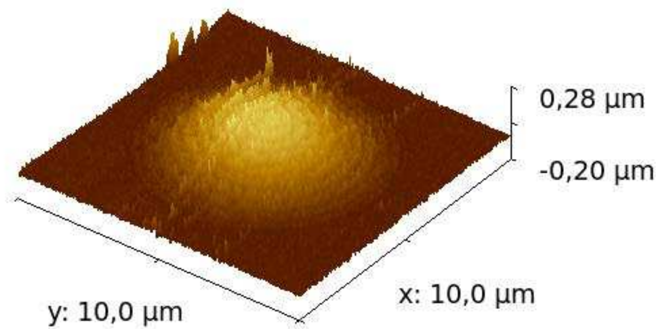

Fig. 12. AFM image of a micro lens created by ion implantation and subsequent RIE pattern transfer

Beside speed, resolution is also among the key properties of a lithographic technique. In the presented lithography technique it is mainly limited by the current distribution of the ion beam and the ion sample interaction. We find that with our Canion 31 Ga LMIS we can easily achieve line/space patterns with 50 nm HP as shown in Fig. 13.

As we have learned, in IBL the proximity effect is absent or negligible. This makes IBL very attractive for 3D nano patterning and possibly the only 3D nano patterning technique with sufficient throughput. The most popular workaround, namely EBL multilevel patterning is a good option if only a few height levels are required. However, it cannot provide real 3D patterns.

We conclude that 3D patterning by ion implantation and subsequent RIE etch is a promising patterning technique. It permits the creation of real 3D nano patterns not feasible with other methods. If combined with nano imprint lithography 3D nano patterns may be economically created and replicated.

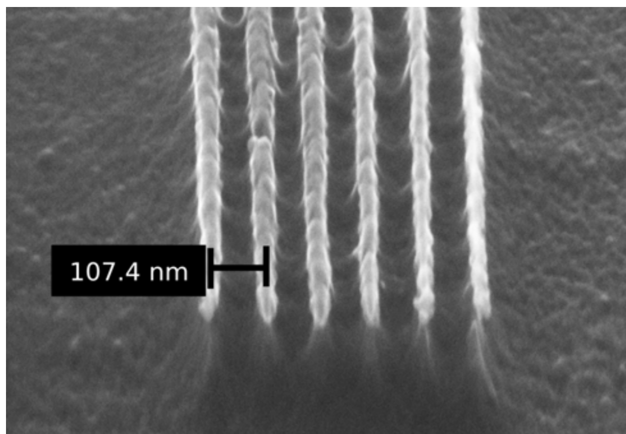

Fig. 13. 50 nm half-pitch lines/spaces. Scanning electron microscope (SEM) image of an implanted and etched lines/spaces pattern with 50 nm half-pitch.

4.4 Direct patterning of hard mask layers

Direct hard mask patterning is an alternative to resist-based patterning and direct FIB milling. To our knowledge, lithography by direct patterning of hard mask layers is a completely new technique.

Compared to resist-based methods, the employment of inorganic mask layers permits a larger flexibility in terms of patterned materials and the patterning of pre-structured substrates with relatively few patterning steps. This technique is not as flexible and straightforward as direct patterning; however, it is significantly faster. Thus, this patterning technique can be seen as a speed/complexity trade-off.

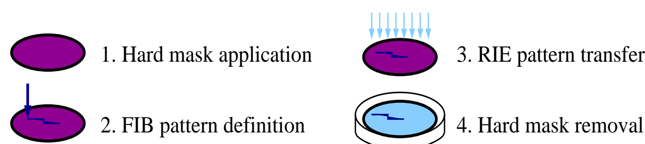

Fig. 14. Process flow for direct hard mask patterning

The direct hard mask patterning technique consists of four steps: (i) Hard mask application, (ii) Pattern definition, (iii) Pattern transfer-etch and (iv) Hard mask removal. For hard mask application standard sputtering, ALD or other methods may be employed. The hard mask removal may be performed in a dedicated etching step, e.g., by wet etching or combined with the RIE pattern transfer step.

For the pattern definition the material properties during FIB patterning are of outstanding importance. Fig. 15 shows the same pattern in two hard mask materials: AZO and Ru on Si. While the pattern in the AZO mask is clearly defined, the pattern in the Ru hard mask is heavily distorted by the surface roughening induced by the FIB milling. In this case, we believe this is due to the formation of Ru island films on the Si substrate.

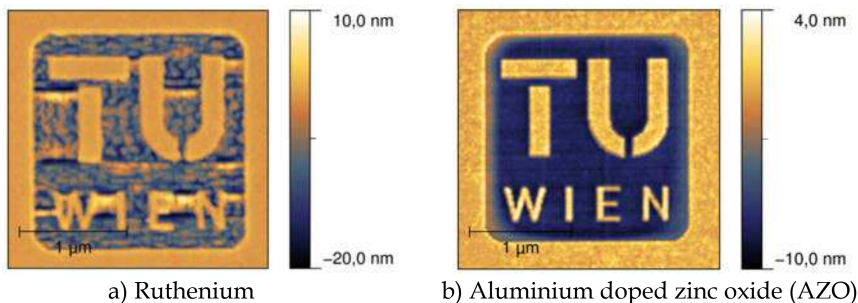

a) Ruthenium b) Aluminium doped zinc oxide (AZO)

Fig. 15. AFM images of two hard materials after pattern definition. The patterning process was identical; however, the resulting pattern quality differs significantly. The nominal hard mask thickness before patterning was 10 nm in both cases.

To quantify the impact of the FIB milling induced roughening, the roughness in dependence of the milling depth was measured for a number of materials. The resulting curves are shown in Fig. 16. Both AZO and Ta masks show excellent flatness after patterning. For Ru, the roughness is found to increase abruptly when the mask thickness approaches zero.

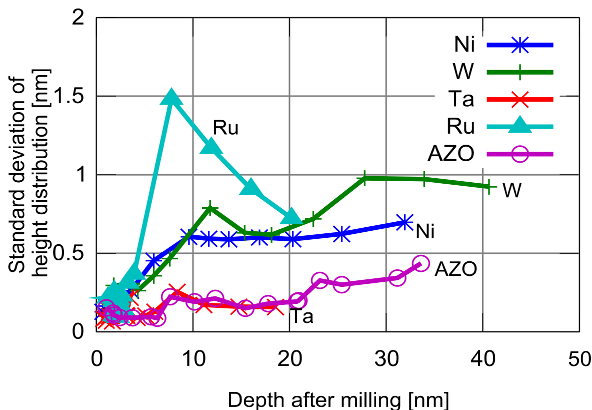

Fig. 16. Impact of ion milling on the roughness of hard mask materials. The hard mask thickness before milling was 10±2 nm in all cases.

For the RIE transfer-etch it is important to choose both the hard mask material and etching chemistry appropriately. Further, it must be considered that during FIB milling the employed ion species is implanted into the substrate and can disturb the etching process. The etching chemistry must etch the substrate material and the implanted ions but must not remove the hard mask material.

Ga implanted into an Si substrate acts as an etch stop for the routinely employed fluorine-based RIE chemistries. We found that our routinely employed Si etch recipes could not be employed for the transfer-etch due to the masking effect of the implanted Ga. Chlorine is known to be an etchant for Ga, thus we investigated the impact of the addition of a chlorine source to a well-established fluorine-based RIE recipe.

The impact of the addition of chlorine on the masking capability of Ga implanted into Si is shown in Fig. 17. While for low $SiCl_4$ concentration the Ga still shows a significant masking effect, we find that the addition of 30% $SiCl_4$ is sufficient to completely suppress the impact of the implanted Ga on the final pattern.

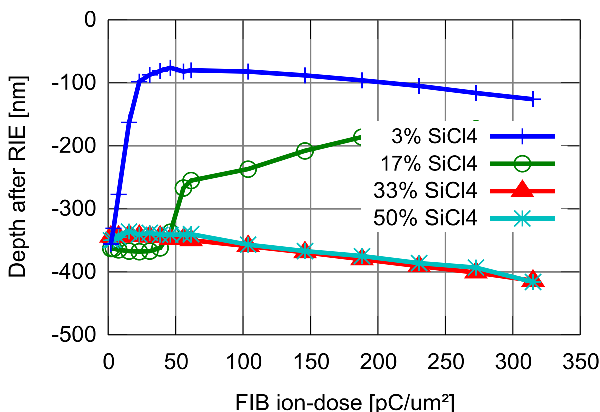

Fig. 17. Impact of the addition of $SiCl_4$ to the masking capability of Ga implanted by FIB into Si in a SF_6-based RIE process

The addition of chlorine solves the issue of Ga implantation. However, it negatively impacts the available pool of hard mask materials. Now the hard mask material must not only resist etching by a standard fluorine-based RIE process but also to the added chlorine species. As shown above, Ta exhibits excellent properties during the pattern definition process. However, it does not resist our chlorine-containing etch recipe and thus cannot be employed.

In terms of resolution, the direct hard mask patterning process compares very favourably to FIB direct milling. Since the pattern in the thin hard mask layer is transferred into a thicker layer, slopes with low steepness are imaged into slopes with higher steepness. Thus patterning close to the beam diameter becomes possible. Also the influence of the beam tails and mechanical deformation due to milling-induced strain is minimized. We found that lines down to 40 nm half pith are obtainable in a 10 nm thick Ni hard mask layer.

We conclude that the direct patterning of hard mask materials and subsequent pattern transfer by RIE can help to speed up patterning compared to direct FIB milling. We believe that this method is useful for a number of applications including patterning on uneven surfaces.

5. Conclusion

Ion beam lithography is a versatile technique with several variations of the process. Single focused ion beams of Ga ions have been successfully used for exposure of resist layers, but more common are direct milling or beam-induced deposition or etching of the material. Also implantation of the ions to pattern surfaces has been demonstrated as a powerful

structuring approach. With the emergence of helium ion beams, a new tool with new structuring capabilities is on the market and allows new applications. In this work also several structuring approaches have been discussed including (i) FIB milling (ii) FIB-induced gas-assisted processes (iii) 3D patterning by ion implantation and (iv) patterning my milling of hard mask layers. Due to the versatility of these approaches an increasing amount of applications of IBL for optical systems, sensor devices, in the modification and custom-trimming of microelectronic circuitry as well as in the 'classical' fields of photomask repair and defect analysis of cross-sections may be expected. With the neon ion beam systems on the verge of commercial introduction, this is surely going to remain an exciting field of research. With the multi-beam ion systems reaching maturity, interest in IBL from the side of industrial fabrication can also be expected in the future.

6. References

Ansari, K. et al., 2004. Fabrication of high aspect ratio 100 nm metallic stamps for nanoimprint lithography using proton beam writing.

Arshak, K. et al., 2004. A novel focused-ion-beam lithography process for sub-100 nanometer technology nodes. *Superlattices and Microstructures*, 36(1-3), pp.335-343.

Bell, D.C. et al., 2009. Precision cutting and patterning of graphene with helium ions. *Nanotechnology*, 20(45), p.455301.

Boit, C. et al., 2008. Physical Techniques for Chip-Backside IC Debug in Nanotechnologies. *Design & Test of Computers, IEEE*, 25(3), pp.250-257.

Calcagno, L., Compagnini, G. & Foti, G., 1992. Structural modification of polymer films by ion irradiation. *Nuclear Inst. and Methods in Physics Research, B*, 65(1-4), pp.413-422.

Chekurov, N. et al., 2009. The fabrication of silicon nanostructures by local gallium implantation and cryogenic deep reactive ion etching. *Nanotechnology*, 20(6).

Choi, J.O. et al., 1988. Degradation of poly(methylmethacrylate) by deep ultraviolet, x-ray, electron beam, and proton beam irradiations. *Journal of Vacuum Science & Technology B: Microelectronics and Nanometer Structures*, 6(6), p.2286.

Dietz, L.A. & Sheffield, J.C., 1975. Secondary electron emission induced by 5–30-keV monatomic ions striking thin oxide films, Journal of Applied Physics, 46(10), 4361.

Driesel, W., Dietzsch, C. & Muhle, R., 1996. In situ observation of the tip shape of AuGe liquid alloy ion sources using a high voltage transmission electron microscope, JVST B, 14(5), 3367.

Dworetsky, S. et al., 1968. Electron Bombardment Ion Source for Low Energy Beams. *Review of Scientific Instruments*, 39(11), p.1721.

Eckstein, W., 1991. *Computer Simulation of Ion-Solid Interactions* 1st ed., Springer.

Giannuzzi, L.A. & Stevie, F.A., 1999. A review of focused ion beam milling techniques for TEM specimen preparation. *Micron*, 30(3), pp.197-204.

Gierak, J. et al., 1997. Focused ion beam nanolithography on AlF_3 at a 10 nm scale. *Applied Physics Letters*, 70(15), p.2049.

Gowa, T. et al., 2010. Ion beam irradiation effects on resist materials. *Journal of Photopolymer Science and Technology*, 23(3), pp.399-404.

Harakawa, K., 1986. Focused ion beam etching of resist materials. *Journal of Vacuum Science & Technology B: Microelectronics and Nanometer Structures*, 4(1), p.355.

Hashimoto, M., 1998. Application of dual-functional MoO_3/WO_3 bilayer resists to focused ion beam nanolithography. *Journal of Vacuum Science & Technology B: Microelectronics and Nanometer Structures*, 16(5), p.2767.

Henry, M.D. et al., 2010. Ga+ beam lithography for nanoscale silicon reactive ion etching. *Nanotechnology*, 21(24).

Hill, R. & Faridur Rahman, F.H.M., 2010. Advances in helium ion microscopy. *Nuclear Instruments and Methods in Physics Research Section A: Accelerators, Spectrometers, Detectors and Associated Equipment*.

Hillmann, M., 2001. *3-dimensionale Nanostrukturierung mittels fokussierter Ionenstrahllithographie*,

Hirscher, S. et al., 2002. Ion projection lithography below 70 nm: tool performance and resist process. *Microelectronic Engineering*, 61-62, pp.301-307.

Horiuchi, K., Itakura, T. & Ishikawa, H., 1988. Fine pattern lithography using a helium field ion source. *Journal of Vacuum Science & Technology B: Microelectronics and Nanometer Structures*, 6(1), p.241.

Hoyle, P., 1994. *Focused electron beam induced chemistry and its application in microelectronics*. University of Cambridge.

Jeon, J., Floresca, H.C. & Kim, M.J., 2010. Fabrication of complex three-dimensional nanostructures using focused ion beam and nanomanipulation. *Journal of Vacuum Science & Technology B: Microelectronics and Nanometer Structures*, 28(3), p.549.

van Kan, Jeroen A., Bettiol, Andrew A. & Watt, Frank, 2006. Proton Beam Writing of Three-Dimensional Nanostructures in Hydrogen Silsesquioxane. *Nano Letters*, 6(3), pp.579-582.

Koeck, A. et al., 2010. Argon ion multibeam nanopatterning of Ni–Cu inserts for injection molding. *Journal of Vacuum Science & Technology B: Microelectronics and Nanometer Structures*, 28(6), p.C6B1.

Kubena, R.L. et al., 1989. Sub-20-nm-wide line fabrication in poly(methylmethacrylate) using a Ga^+ microprobe. *Journal of Vacuum Science & Technology B: Microelectronics and Nanometer Structures*, 7(6), p.1798.

Lee, H.-Y. & Chung, H.-B., 1998. Ga+ focused-ion-beam exposure and CF4 reactive-ion-etching development of Si_3N_4 resist optimized by Monte Carlo simulation, JVST B, 16(3), 1161.

Livengood, R.H. et al., 2011. The neon gas field ion source--a first characterization of neon nanomachining properties. *Nuclear Instruments and Methods in Physics Research Section A: Accelerators, Spectrometers, Detectors and Associated Equipment*, In Press, Corrected Proof.

Loeschner, Hans, Klein, C. & Platzgummer, Elmar, 2010. Projection Charged Particle Nanolithography and Nanopatterning. *Japanese Journal of Applied Physics*, 49(6), p.06GE01.

Matsui, S. et al., 2000. Three-dimensional nanostructure fabrication by focused-ion-beam chemical vapor deposition, JVST B, 18(6), 3181.

Melngailis, J., 1993. Focused ion beam lithography. *Nuclear Inst. and Methods in Physics Research, B*, 80-81(PART 2), pp.1271-1280.

Muehlberger, M. et al., 2011. Nanoimprint lithography from CHARPAN Tool exposed master stamps with 12.5 nm hp. *Microelectronic Engineering*, In Press, Corrected Proof.

Namatsu, H. et al., 1998. Nano-patterning of a hydrogen silsesquioxane resist with reduced linewidth fluctuations. *Microelectronic Engineering*, 41-42, pp.331-334.

Notte, J., 4th et al., 2010. Diffraction imaging in a He+ ion beam scanning transmission microscope. *Microscopy and Microanalysis: The Official Journal of Microscopy Society of America, Microbeam Analysis Society, Microscopical Society of Canada*, 16(5), pp.599-603.

Orloff, J., Swanson, L.W. & Utlaut, M., 1996. Fundamental limits to imaging resolution for focused ion beams. *Journal of Vacuum Science & Technology B: Microelectronics and Nanometer Structures*, 14(6), p.3759.

Orloff, J., Swanson, L. & Utlaut, Mark, 2002. *High Resolution Focused Ion Beams: FIB and Applications* 1st ed., Springer.

Persson, A., Thornell, G. & Nguyen, H., 2010. Rapid prototyping of magnetic tunnel junctions with focused ion beam processes. *Journal of Micromechanics and Microengineering*, 20(5).

Platzgummer, Elmar & Loeschner, Hans, 2009. Charged particle nanopatterning. *Journal of Vacuum Science & Technology B: Microelectronics and Nanometer Structures*, 27(6), p.2707.

Rau, N., 1998. Shot-noise and edge roughness effects in resists patterned at 10 nm exposure. *Journal of Vacuum Science & Technology B: Microelectronics and Nanometer Structures*, 16(6), p.3784.

Reyntjens, S. & Puers, R., 2001. A review of focused ion beam applications in microsystem technology. *Journal of Micromechanics and Microengineering*, 11(4), pp.287-300.

Schmidt, B., Bischoff, L. & Teichert, J., 1997. Writing FIB implantation and subsequent anisotropic wet chemical etching for fabrication of 3D structures in silicon. *Sensors and Actuators A: Physical*, 61(1-3), pp.369-373.

Sidorkin, V. et al., 2009. Sub-10-nm nanolithography with a scanning helium beam. *Journal of Vacuum Science & Technology B: Microelectronics and Nanometer Structures*, 27(4), p.L18.

Taniguchi, J. et al., 2006. Rapid and three-dimensional nanoimprint template fabrication technology using focused ion beam lithography. *Microelectronic Engineering*, 83(4-9), pp.940-943.

Tseng, A.A., 2004. Recent developments in micromilling using focused ion beam technology. *Journal of Micromechanics and Microengineering*, 14(4), p.R15-R34.

Tseng, A.A., 2005. Recent Developments in Nanofabrication Using Focused Ion Beams. *Small*, 1(10), pp.924-939.

Utke, I., Hoffmann, P. & Melngailis, John, 2008. Gas-assisted focused electron beam and ion beam processing and fabrication. *Journal of Vacuum Science & Technology B: Microelectronics and Nanometer Structures*, 26(4), p.1197.

Wagner, A., 1981. Germanium selenide: A resist for low-energy ion beam lithography. *Journal of Vacuum Science and Technology*, 19(4), p.1363.

Ward, B.W., Notte, J.A. & Economou, N.P., 2006. Helium ion microscope: A new tool for nanoscale microscopy and metrology. *Journal of Vacuum Science & Technology B: Microelectronics and Nanometer Structures*, 24(6), p.2871.

Winston, D. et al., 2009. Scanning-helium-ion-beam lithography with hydrogen silsesquioxane resist. *Journal of Vacuum Science and Technology B: Microelectronics and Nanometer Structures*, 27(6), pp.2702-2706.

Yasaka, A. et al., 2008. Application of vector scanning in focused ion beam photomask repair system. *Journal of Vacuum Science and Technology B: Microelectronics and Nanometer Structures*, 26(6), pp.2127-2130.
Ziegler, J.F., 2004. SRIM-2003. *Nuclear Instruments and Methods in Physics Research, Section B: Beam Interactions with Materials and Atoms*, 219-220(1-4), pp.1027-1036.

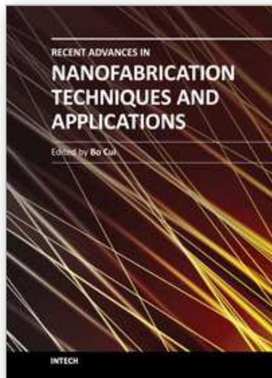

Recent Advances in Nanofabrication Techniques and Applications
Edited by Prof. Bo Cui

ISBN 978-953-307-602-7
Hard cover, 614 pages
Publisher InTech
Published online 02, December, 2011
Published in print edition December, 2011

Nanotechnology has experienced a rapid growth in the past decade, largely owing to the rapid advances in nanofabrication techniques employed to fabricate nano-devices. Nanofabrication can be divided into two categories: "bottom up" approach using chemical synthesis or self assembly, and "top down" approach using nanolithography, thin film deposition and etching techniques. Both topics are covered, though with a focus on the second category. This book contains twenty nine chapters and aims to provide the fundamentals and recent advances of nanofabrication techniques, as well as its device applications. Most chapters focus on in-depth studies of a particular research field, and are thus targeted for researchers, though some chapters focus on the basics of lithographic techniques accessible for upper year undergraduate students. Divided into five parts, this book covers electron beam, focused ion beam, nanoimprint, deep and extreme UV, X-ray, scanning probe, interference, two-photon, and nanosphere lithography.

How to reference
In order to correctly reference this scholarly work, feel free to copy and paste the following:

Heinz D. Wanzenboeck and Simon Waid (2011). Focused Ion Beam Lithography, Recent Advances in Nanofabrication Techniques and Applications, Prof. Bo Cui (Ed.), ISBN: 978-953-307-602-7, InTech, Available from: http://www.intechopen.com/books/recent-advances-in-nanofabrication-techniques-and-applications/focused-ion-beam-lithography

INTECH
open science | open minds

InTech Europe
University Campus STeP Ri
Slavka Krautzeka 83/A
51000 Rijeka, Croatia
Phone: +385 (51) 770 447
Fax: +385 (51) 686 166
www.intechopen.com

InTech China
Unit 405, Office Block, Hotel Equatorial Shanghai
No.65, Yan An Road (West), Shanghai, 200040, China
中国上海市延安西路65号上海国际贵都大饭店办公楼405单元
Phone: +86-21-62489820
Fax: +86-21-62489821

© 2011 The Author(s). Licensee IntechOpen. This is an open access article distributed under the terms of the Creative Commons Attribution 3.0 License, which permits unrestricted use, distribution, and reproduction in any medium, provided the original work is properly cited.